Walisongo Journal of Chemistry
Walisongo Journal of Chemistry Vol. 6 Issue 1 (2023), 61-68
ISSN: 2621-5985 (online); 2549-385X (print)
DOI: https://doi.org/10.21580/wjc.v6i1.15696

Molecular Modelling Based on TD-DFT Applied to UV Spectra of Coumarin Derivatives

Mokhamat Ariefin*, Rokiy Alfanaar

Department of Chemistry, Faculty of Mathematic and Sciences, University of Palangka Raya, Yos Sudarso Street, Palangka Raya City, Indonesia

*corresponding author: mokhamatariefin@mipa.upr.ac.id

Received: 12 April 2023; Accepted: 1 July 2023; Published: 25 July 2023

Abstract

The optimization of geometry and electronic transition of seven coumarin derivatives for sunscreen activity have been conducted using Orca. DFT methods is applied to find optimum geometry and parameter data is measured like bond length and bond angle. TD-DFT is conducted to get electronic transition to get ultraviolet (UV) spectra. The result shows that the coumarin derivative transition type is n to π and π to π*. All coumarin exhibits the properties of UV-B protection, however, two out of seven show properties as a UV-A protection. The energy difference HOMO-LUMO shows that coumarin with isopropyl substituent has the smallest energy gap, around 0.1559, whereas coumarin with fluorine atom substituent has the biggest energy gap.*

Keywords: *coumarin; sunscreen; TD-DFT; energy gap*

Introduction

Ultraviolet (UV) radiation is classified into three categories based on their wavelength range. The type of UV radiation is UV-C in the range 100-280 nm, UV-B in the range 280-320 nm, and UV-A in the range 320-400 nm (Zam et al., 2018). In human, UV provides a benefit for human healts in terms of the synthesis of vitamin D. Vitamin D is 80% synthesized in the presence of UV rays from sunlight (Wimalawansa et al., 2018). However, several studies also reported that sunlight exposure to humans has some negative effects. The UV-B radiation can penetrate through the atmosphere of the earth and then absorbed by photosensitive macromolecules in human body such as protein, RNA, or DNA that result in alternation in their chemical structure (Holick, 2016). UV exposure will increase the risk of long-term damage such as photo aging, pigmentary changes, wrinkling, malignancy, athropy, and skin cancer (D'Orazio et al., 2013; Narayanan et al., 2010; Panich et al., 2016). Carr et al., (2020), also reported that UV irradiation also affects indirect mutational role in promoting melanoma and oncogene induction as well as an indirect role through micro-environmental alternation. Therefore, the use of skin protection against UV irradition needs to be considered.

Sunscreen or UV protection are chemical compounds that can be employed as a photo-protectant against UV rays. The demand for sunscreen products increases consistent to higher awareness of people about the increasing cases of UV induced melanoma (Geoffrey et al., 2019). The UV

Copyright © 2023 WJC | ISSN 2621-5985 (online) | ISSN 2549-385X (print)

protection material can be produced both from anorganic and organic materials. Inorganic sunscreen materials are inorganic material reflect UV ray from protected (Yuan et al., 2022). The common material that has been used as sunscreen is ZnO_2 and TiO_2, however, ZnO_2 produced a substansial amount of reactive oxygen species (ROS) during the UV-A exposure (Lewicka et al., 2013). On the other hand, organic sunscreen is organic material that can protect protected areas from UV rays. The plant extract has been discovered to evaluate the sunscreen properties (Cefali, 2019; Morocho-Jácome, 2021).

Organic sunscreen generally consists of oganic compound linked with carbonyl group. In other hand, the organic active material of sunscreens can also build from a combination of chromophore and auxochrome groups that can absorb a specific wavelength in UV range, such as derivates of benzophenone, aminobenzoate, and cinnamic acid (Aziz et al., 2019; Gunia-Krzyżak et al., 2018; Kim & Choi, 2014). Sunscreen activity is generally studied through the relationship of intensty to wavelength using UV instrument or in vivo tests with high exposure of UV radiation to calculate sun protection factor (SPF) (Cole et al., 2019).

On the other hand, the properties of sunscreen properties can be studied by computational modeling. The UV protection properties can be evaluated through the relationship between intensity and wavelength (Hadi, 2016). Modern quantum chemistry approaches provide a valuable and powerful approach based on time-dependent – density functional theory (TD-DFT), which is widely used to predict the absorption spectra of UV-visible (vis) - near infrared (NIR) from organic, inorganic, or organometal compounds (Martynov et al., 2017, 2019).

Coumarin is a second metabolite product widespread in nature that can be found in plants, fungi, or bacteria. Coumarin is a bicyclic heteroatom consisting of two oxygen atoms, one in the ring and another in the carbonyl group (Annunziata et al., 2020). The structure of coumarin is available in figure 1. Research of coumarin has been widely spread in various fields, such as chemosensor or cancer therapeutic (Annunziata et al., 2020). Coumarin is also reported to have UV protection activity (Cao, 2019). Based on that report, this study aims to get optimum structure modeling of coumarin derivatives as a sunscreen. The modeling object are seven coumarin derivatives (**1-7**) with different electron-donating group in C7 of coumarin. This article will report the potential of coumarin derivatives as sunscreen through electronic transition modeling. Electron transition of coumarin derivatives will describe the energy required when subjected to light. The determination of transition electron also exhibits the high occupied molecular orbital (HOMO) level and low unoccupied molecular orbital (LUMO) energy level, which affect the potential as a sunscreen. Furthermore, this study's outcome will guide the development of the synthesis of sunscreen material for food, medicine, or cosmetics.

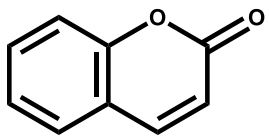

Figure 1. Structure of coumarin

Methods

This experiment was conducted using laptop with processor Intel® CoreTM i5-7200U, CPU @2.50 GHz, and 8 GB RAM. The software: Orca 4.2.1 for calculation and Avogadro for drawing structure of compound, IboView to interpret HOMO-LUMO depiction. ChemBioDraw Ultra 14.0 was used to draw chemical structures of coumarin derivatives.

Computational calculation using Density Functional Theory (DFT) for geometry optimization and Time-Dependent Density Functional Theory (TD-DFT) for energy calculations. The geometry optimization calculation was using basis set B3LYP def2-SVP by Orca. The geometry modelling

Copyright © 2023 WJC | ISSN 2621-5985 (online) | ISSN 2549-385X (print)

optimization was set in the gas phase. The materials of this research are seven derivatives compounds from coumarin. The structure of the compound is available at **table 1**. The properties to be obtained for this experiment are structural parameters, dipole moment, atomic charge, HOMO-LUMO, and energy gap.

Table 1. Stucture of coumarin derivative

No	Compound name	Structure
1	7-hydroxycoumarin	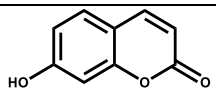
2	7-methyoxycoumarin	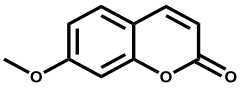
3	7-ethoxycoumarin	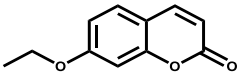
4	7-propoxycoumarin	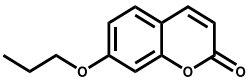
5	7-isopropoxycoumarin	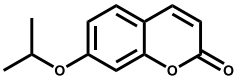
6	7-allyloxycoumarin	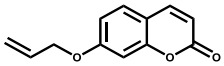
7	7-fluorocoumarin	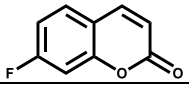

Result and Discussion

Geometry Optimization of Comarine Derivatives

The optimization of the molecular geometry of coumarin derivatives compound conducted by DFT methods basis def2-SVP. The strcuture of coumarin derivatives was different in the alkoxy group (methoxy, ethoxy, propoxy, isopropoxy), alkene, and fluorine atom. Geometry optimization can exhibit the stability of a molecule, so the model of molecular structure is closer to the actual molecule. The optimized geometry of coumarin derivatives is available at **table 2**.

Table 2. Three-dimensional optimazation geometry of coumarin derivative

3D structure	3D structure
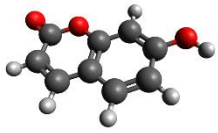 **1**	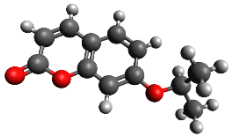 **5**
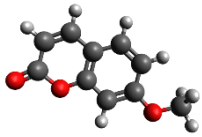 **2**	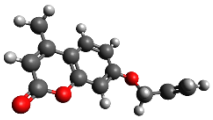 **6**
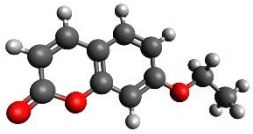 **3**	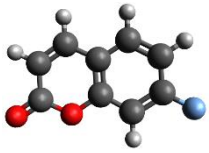 **7**
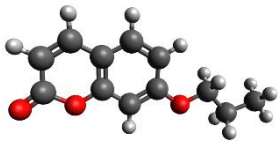 **4**	

The molecular geometry optimization will describe the effect of the substituent on the term of bond length and bond angle. The molecular structure with label and data of bond length and bond angle of coumarin derivatives **1-7** is available in **figure 2** and **table 3**. In this research, the bond length of the benzene ring in the coumarin structures does not significantly affect in the presence of an alkyl group **(1-6)**, or fluorine atom **(7)**. The bond angle between carbon atom (C6), oxygen atom, and the substituent (alkyl group, amino, or fluorine atom) not significantly change. The bond angle with alkoxy group (compound **2-6**) is larger than hidroxy group (compound **1**) because the presence of alkyl group will increase the electronic repulsion. Among the alkoxy group substituent, compound **5** has the biggest bond angle because the isopropyl chain has a bulky structure than straight chain alkyl.

Copyright © 2023 WJC | ISSN 2621-5985 (online) | ISSN 2549-385X (print)

Table 3. Three dimensional optimization geometry of coumarin derivative

Optimized Geometry	atom	Compound 1	2	3	4
Bond Length (A)	C1-C2	1.413	1.427	1.427	1.427
	C2-C4	1.400	1.399	1.399	1.399
	C4-C6	1.401	1.410	1.411	1.411
	C6-C7	1.404	1.421	1.421	1.421
	C7-C3	1.398	1.397	1.397	1.397
	C3-C1	1.401	1.415	1.415	1.415
	C6-O2	1.358	1.358	1.357	1.357
Bond Angle (°)	$C_{1,2,4}$	119.8	121.6	121.6	121.6
	$C_{2,4,6}$	120.2	119.6	119.6	119.5
	C_6, O_2, R	109.0	119.1	119.6	119.7

Optimized Geometry	atom	Compound 5	6	7
Bond Length (A)	C1-C2	1.427	1.422	1.392
	C2-C4	1.399	1.407	1.393
	C4-C6	1.412	1.408	1.393
	C6-C7	1.423	1.423	1.397
	C7-C3	1.396	1.389	1.398
	C3-C1	1.415	1.421	1.397
	C6-O2	1.357	1.357	
	C6-F			1.339
Bond Angle (°)	$C_{1,2,4}$	121.7	121.7	121.7
	$C_{2,4,6}$	119.6	119.2	119
	C_6, O_2, R	121.4	119.1	-

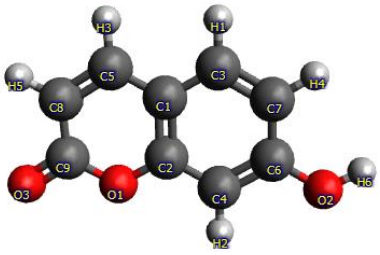

Figure 2. The structure of coumarin derivative (7-hydroxycoumarin) with labeling.

Dipole Moment and Atomic Charge of Optimized Geometry

The molecular dipole moment is a quantity that provides essential insight into the distribution of the electron charge in the multiatomic compound and measures the amount of a molecule's polarity. The dipole moment of the compound can be determined with some main principles, such as given chemical bond and their mutual arrangement. On a simplified level, in a multiatomic molecule like coumarin, the dipole moment can be considered as a of a geometric summation of the individual moment of each bond in the molecules. The dipole moment data for all coumarin derivatives is available in table 4. The presence of the alkyl group in compound 2-5 will decrease the dipole moment, but not but the long of chain in the alkyl group do not give a significant difference. However, the presence of the higher electronegativity group, such as the alkene group (compound 6) or fluorine atom (compound 7) will decrease the moment dipole significantly. The Alkene group in compound 6 has higher electronegativity than alkyl group in compound 2-5. The electronegativity of the carbon chain depends on hybridization of the orbital. Greater s character of the hybridization will increase the electronegativity. The dipole moment of compound 7 is slightly different from compounds 6 due to the presence of fluorine. Fluorine is an atom with the highest electronegativity in the periodic table.

The TD-DFT method also can calculate the atomic charge of the compound because it assumes an electron as an electron cloud with a density unit, not as a single particle. The atomic charge analysis was carried out to explain the effect of the substituent on the atomic charge distribution of the coumarin derivative compounds. Atomic charge analysis is used to analyze the effect of substituents on distribution patterns on coumarin derivatives. The atomic charge of coumarin derivatives is available in table 5. The data shows that the atomic charge in C6 is positive for all coumarin derivatives due to the presence of an electronegative atom. In contrast, the charge of C4 and C7 of all coumarin derivatives have a negative charge. The total charge of the benzene ring is slightly negative because the presence of -OR (alkoxy) or -F (fluorine) group will pull the electron moiety in benzene to the outside of the ring.

Copyright © 2023 WJC | ISSN 2621-5985 (online) | ISSN 2549-385X (print)

Table 4. The dipole moment of derivate of coumarin

Compound	Dipole Moment (Debye)	Compound	Dipole Moment (Debye)
1	7.08	**5**	6.66
2	6.38	**6**	4.45
3	6.47	**7**	4.84
4	6.53		

Table 5. Atomic charge of coumarin dervatives

Atomic Position	Compound/Atomic Charge						
	1	**2**	**3**	**4**	**5**	**6**	**7**
C1	0.12	0.095	0.095	0.093	0.083	0.077	0.14
C2	0.28	0.31	0.30	0.31	0.30	0.24	0.25
C3	-0.24	-0.23	-0.24	-0.24	-0.24	-0.19	-0.21
C4	-0.32	-0.34	-0.35	-0.37	-0.35	-0.32	-0.33
C6	0.34	0.38	0.38	0.39	0.39	0.37	0.39
C7	-0.19	-0.24	-0.23	-0.23	-0.23	-0.20	-0.20
O2	-0.40	-0.26	-0.25	-0.25	-0.27	-0.25	
F							-0.19

The electronic transition modeling was performed using the TD-DFT method. The data parameter taken by this method is HOMO-LUMO energy level, wavelength, and intensity. All this data was used to study the anti-UV activity of coumarin derivatives. The UV intensity calculation of coumarin derivatives 1-7 was conducted to learn their optical properties in the UV region (200-400 nm). Figure 3 shows the result of the theoretical UV absorption calculation. Figure 3 shows the presence of methyl group in compounds 2-6, slightly giving a redshift to the λmax compared to compound 1. The presence of another electron donating like fluorine, also gives redshift to coumarin λmax. The transition occurs on coumarin derivatives on UV range shown in n to π* transition by adding π to π* transition. The coumarin spectra in UV range don't show individual line n to π* transition. Transition n to π* occurs because there are nonbonding electrons located on the oxygen carbonyl group of coumarin. Thus, the n to π* transition corresponds to the excitation of an electron from one f the unshared pair to the π* orbital. Transition π to π* exhibits the substitution group, which is an auxochrome group, which can influence the wavelength shift. The UV absorption spectra of compounds 1-7 show that all compounds indicate the potential for anti-UV activity in the UV B (280-325 nm). However, only compounds 1 and 6 that show potential for anti-UV in the UV-C because these compounds have absorption in the range 100-280 nm.

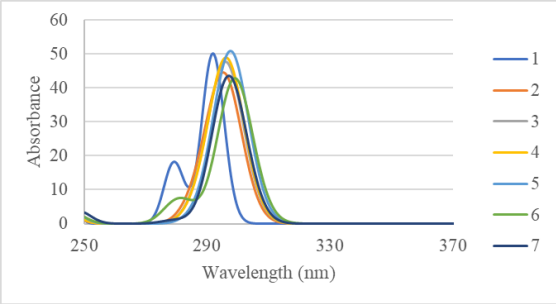

Figure 3. Absorption spectra of coumarin derivatives based on computational calculations.

Energy Gap of Coumarin Derivatives

The other parameter measured in the study of the anti-UV of coumarin derivatives is HOMO and LUMO energy level. The highest occupied molecular orbital (HOMO) is the highest energy level of molecular orbital filled with electrons. The lowest unoccupied molecular orbital (LUMO) is the lowest molecular energy level that is not filled by electrons. The energy difference between HOMO and LUMO, known as the energy gap (Egap¬), is the minimum energy required to excite electrons from HOMO to LUMO. The energy gap HOMO-LUMO of a compound exhibit how to ease the electron excited when a compound is subjected to electromagnetic radiation.

Modeling of HOMO-LUMO energy level was carried out using TD-DFT and interpreted using IboVIew. The result of the interpretation of the HOMO and LUMO of coumarin derivative is available in table 6 and table 7, furthermore the energy gap is available in table 8. The results show that the presence of strong electron-donating group (or more electronegative atom) will increase

Copyright © 2023 WJC | ISSN 2621-5985 (online) | ISSN 2549-385X (print)

both HOMO and LUMO levels of the compound. Compound 7 has the highest HOMO and LUMO energy level than the other coumarin derivatives. The energy gap of compounds 1-7 is slightly different. However, compound 5 exhibits the lowest energy gap (Eg (LUMO/HOMO).

Table 6. HOMO Energy Level of Coumarin Derivatives

	HOMO-1 (eV)	HOMO (eV)
1	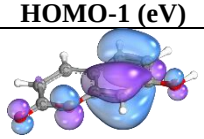 -0.2641	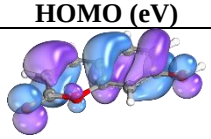 -0.2302
2	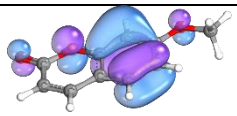 -0.2565	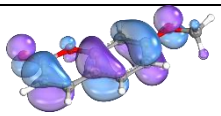 -0.2316
3	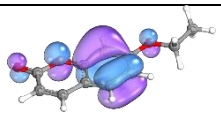 -0.2550	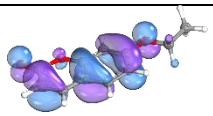 -0.2300
4	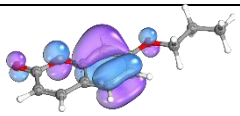 -0.2546	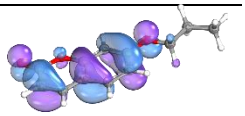 -0.2296
5	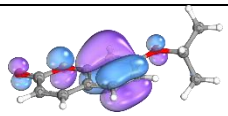 -0.2539	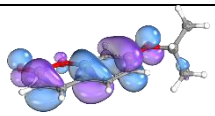 -0.2277
6	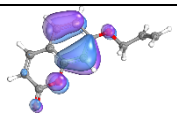 -0.2605	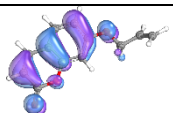 -0.2293
7	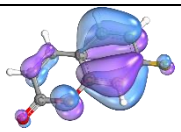 -0.2774	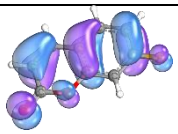 -0.2543

Table 7. LUMO Energy Level of Coumarin Derivatives

	LUMO (eV)	LUMO+1 (eV)
1	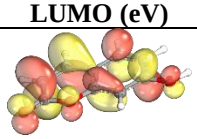 -0.0741	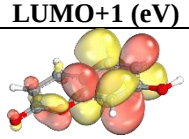 -0.0337
2	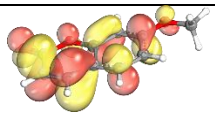 -0.0745	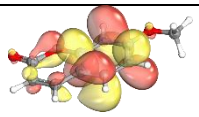 -0.0276
3	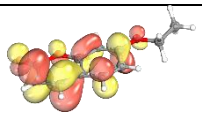 -0.0732	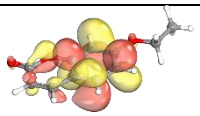 -0.0262
4	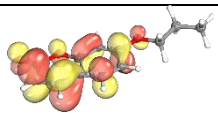 -0.0729	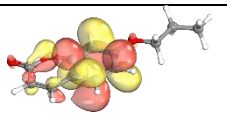 -0.0258
5	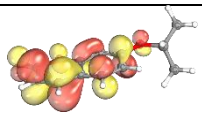 -0.0718	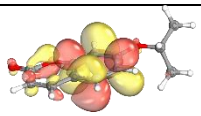 -0.0252
6	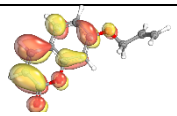 -0.0730	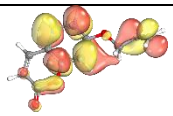 -0.0296
7	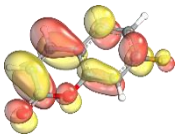 -0.0797	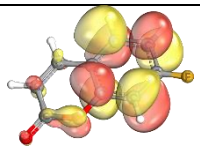 -0.0431

Table 8. Energy gap coumarin derivatives

	Energy Gap (eV)			
	E_g (LUMO/HOMO-1)	E_g (LUMO/HOMO)	E_g (LUMO+1/HOMO-1)	E_g (LUMO+1/HOMO)
1	0.1900	0.1561	0.2304	0.1965
2	0.1820	0.1571	0.2289	0.2040
3	0.1818	0.1568	0.2288	0.2038
4	0.1817	0.1567	0.2288	0.2038
5	0.1821	0.1559	0.2287	0.2025
6	0.1875	0.1563	0.2309	0.1997
7	0.1977	0.1746	0.2343	0.2112

Copyright © 2023 WJC | ISSN 2621-5985 (online) | ISSN 2549-385X (print)

Conclusion

The molecular geometry of optimization of coumarin derivative was carried out using DFT methods to get the stable structure of coumarin derivative (**1-7**). The determination of electronic transition using TD-DFT methods shows each coumarin derivative shows activity as a sunscreen activity. Compounds 1 and 6 show the potential to become UV-C protection material. Conversely, compound **1-7** exhibits the potential to be a UV-B protection material. Compound **7** has the highest HOMO and LUMO level due to the presence of a strong electron-donating group. Compound 5 has the best potential than the other coumarin derivative because it has the lowest E_g HOMO-LUMO.

Reference

Annunziata, F., Pinna, C., Dallavalle, S., Tamborini, L., & Pinto, A. (2020). An Overview of Coumarin as a Versatile and Readily Accessible Scaffold with Broad-Ranging Biological Activities. *Int J Mol Sci*, *21*(13), 4618. https://doi.org/10.3390/ijms21134618.

Aziz, I. N. F. A., Sarijo, S. H., Rajidi, F. S. M., Yahaya, R., & Musa, M. (2019). Synthesis and characterization of novel 4-aminobenzoate interleaved with zinc layered hydroxide for potential sunscreen application. *Journal of Porous Materials*, *26*(3), 717–722,. https://doi.org/10.1007/s10934-018-0668-2.

Cao, D. (2019). Coumarin-Based Small-Molecule Fluorescent Chemosensors. *Chem Rev*, *119*(18), 10403–10519,. https://doi.org/10.1021/acs.chemrev.9b00145.

Carr, S., Smith, C., & Wernberg, J. (2020). Epidemiology and Risk Factors of Melanoma. *Surgical Clinics of North America*, *100*(1), 1–12,. https://doi.org/10.1016/j.suc.2019.09.005.

Cefali. (2019). Flavonoid-Enriched Plant-Extract-Loaded Emulsion: A Novel Phytocosmetic Sunscreen Formulation with Antioxidant Properties. *Antioxidants*, *8*(10), 443. https://doi.org/10.3390/antiox8100443.

Cole, C., Silverman, J., & Bonitatibus, M. (2019). Evaluating sunscreen ultraviolet protection using a polychromatic diffuse reflectance device. *Photodermatol Photoimmunol Photomed*, *35*(6), 436–441,. https://doi.org/10.1111/phpp.12496.

D'Orazio, J., Jarrett, S., Amaro-Ortiz, A., & Scott, T. (2013). UV Radiation and the Skin. *Int J Mol Sci*, *14*(6), 12222–12248,. https://doi.org/10.3390/ijms140612222.

Geoffrey, K., Mwangi, A. N., & Maru, S. M. (2019). Sunscreen products: Rationale for use, formulation development and regulatory considerations. *Saudi Pharmaceutical Journal*, *27*(7), 1009–1018,. https://doi.org/10.1016/j.jsps.2019.08.003.

Gunia-Krzyżak, A., Słoczyńska, K., Popiół, J., Koczurkiewicz, P., Marona, H., & Pękala, E. (2018). Cinnamic acid derivatives in cosmetics: current use and future prospects. *Int J Cosmet Sci*, *40*(4), 356–366,. https://doi.org/10.1111/ics.12471.

Hadi, A. (2016). Quantum-Chemical Study For Some Coumarin Compounds by using semi-empirical methods. *Int J Chemtech Res*, *9*(Feb.), 139–148.

Holick, M. F. (2016). *Biological Effects of Sunlight, Ultraviolet Radiation, Visible Light, Infrared Radiation and Vitamin D for Health*.

Kim, S., & Choi, K. (2014). Occurrences, toxicities, and ecological risks of benzophenone-3, a common component of organic sunscreen

Copyright © 2023 WJC | ISSN 2621-5985 (online) | ISSN 2549-385X (print)

products: A mini-review. *Environ Int*, *70*(Sept.), 143–157,. https://doi.org/10.1016/j.envint.2014.05.015.

Lewicka, Z. A., Yu, W. W., Oliva, B. L., Contreras, E. Q., & Colvin, V. L. (2013). Photochemical behavior of nanoscale TiO2 and ZnO sunscreen ingredients. *J Photochem Photobiol A Chem*, *263*, 24–33,. https://doi.org/10.1016/j.jphotochem.2013.04.019.

Martynov, A. G., Mack, J., May, A. K., Nyokong, T., Gorbunova, Y. G., & Tsivadze, A. Y. (2019). Methodological Survey of Simplified TD-DFT Methods for Fast and Accurate Interpretation of UV–Vis–NIR Spectra of Phthalocyanines. *ACS Omega*, *4*(4), 7265–7284,. https://doi.org/10.1021/acsomega.8b03500.

Martynov, A. G., Mack, J., Ngoy, B. P., Nyokong, T., Gorbunova, Y. G., & Tsivadze, A. Y. (2017). Electronic structure and NH-tautomerism of a novel metal-free phenanthroline-annelated phthalocyanine. *Dyes and Pigments*, *140*(May), 469–479,. https://doi.org/10.1016/j.dyepig.2017.01.072.

Morocho-Jácome, A. L. (2021). In vivo SPF from multifunctional sunscreen systems developed with natural compounds—A review. *J Cosmet Dermatol*, *20*(3), 729–737,. https://doi.org/10.1111/jocd.13609.

Narayanan, D. L., Saladi, R. N., & Fox, J. L. (2010). Review: Ultraviolet radiation and skin cancer. *Int J Dermatol*, *49*(9), 978–986,. https://doi.org/10.1111/j.1365-4632.2010.04474.x.

Panich, U., Sittithumcharee, G., Rathviboon, N., & Jirawatnotai, S. (2016). Ultraviolet Radiation-Induced Skin Aging: The Role of DNA Damage and Oxidative Stress in Epidermal Stem Cell Damage Mediated Skin Aging. *Stem Cells Int*, *2016*, 1–14,. https://doi.org/10.1155/2016/7370642.

Wimalawansa, S. J., Razzaque, M. S., & Al-Daghri, N. M. (2018). Calcium and vitamin D in human health: Hype or real? *J Steroid Biochem Mol Biol*, *180*, 4–14,. https://doi.org/10.1016/j.jsbmb.2017.12.009.

Yuan, S., Huang, J., Jiang, X., Huang, Y., Zhu, X., & Cai, Z. (2022). Environmental Fate and Toxicity of Sunscreen-Derived Inorganic Ultraviolet Filters in Aquatic Environments: A Review. *Nanomaterials*, *12*(4), 699. https://doi.org/10.3390/nano12040699.

Zam, Z., Juniyanti, D., & Rakhman, K. (2018). Effectivity Of Ethanolic Extracts From Jambulang Fruit (Syzigium Cumini. L) As Ultraviolet Anti Radiation Agent. *Int J Adv Res (Indore*, *6*(4), 949–954,. https://doi.org/10.21474/IJAR01/6933.

Copyright © 2023 WJC | ISSN 2621-5985 (online) | ISSN 2549-385X (print)